Chinese Chemical Letters 37 (2026) 110588

Contents lists available at ScienceDirect

Chinese Chemical Letters

journal homepage: www.elsevier.com/locate/cclet

From $HgGa_2(SeO_3)_4$ to $Hg_2Ga(SeO_3)_2F$: The first Hg^I-based selenite birefringent crystal triggered by linear groups and fluoride ions

Peng-Fei Li[a,b], Chun-Li Hu[a,b], Bo Zhang[a,b], Jiang-Gao Mao[a,b], Fang Kong[a,b,*]

[a] State Key Laboratory of Structural Chemistry, Fujian Institute of Research on the Structure of Matter, Chinese Academy of Sciences, Fuzhou 350002, China
[b] University of Chinese Academy of Sciences, Beijing 100049, China

ARTICLE INFO

Article history:
Received 2 October 2024
Revised 23 October 2024
Accepted 29 October 2024
Available online 3 November 2024

Keywords:
Optical properties
Crystal structures
Selenites
Birefringence
Nonlinear optical

ABSTRACT

Exploring new material systems and enhancing the birefringence of compounds is a highly valuable endeavor. In this study, we introduce a novel method to enhance the birefringence of inorganic compounds by inducing structural alignment through linear groups and fluoride ions. We report on two new compounds: $HgGa_2(SeO_3)_4$ and $Hg_2Ga(SeO_3)_2F$. $HgGa_2(SeO_3)_4$ crystallizes in a non-centrosymmetric (NCS) space group, exhibiting a second harmonic generation (SHG) efficiency of approximately 60% that of commercial KH_2PO_4 (KDP), with a birefringence of 0.032@546 nm. $Hg_2Ga(SeO_3)_2F$, on the other hand, crystallizes in a centrosymmetric space (CS) group and represents the first reported Hg^I-based selenite birefringent material. Due to the influence of the linear group Hg_2O_2, its birefringence is significantly enhanced to 0.111@546 nm, which is 3.5 times that of $HgGa_2(SeO_3)_4$. Moreover, both compounds demonstrate high stability and a broad optical transparency window. These findings indicate that $Hg_2Ga(SeO_3)_2F$ is a promising candidate for birefringent material in the mid-infrared (MIR) range. Our research provides an innovative strategy for improving the birefringence of compounds.

© 2025 Published by Elsevier B.V. on behalf of Chinese Chemical Society and Institute of Materia Medica, Chinese Academy of Medical Sciences.

Birefringent crystals are important optical functional components in commercial, agricultural, industrial, and military fields [1–4]. Some crystals have been commercialized, such as $CaCO_3$ [5], YVO_4 [6], MgF_2 [7], TiO_2 [8], and $LiNbO_3$ [9]. In recent years, the requirements for miniaturization of devices have also increased, with the rapid development of photoelectric technology. The miniaturization of devices requires that crystals must have sufficiently large birefringence [10–12]. Therefore, it is very important to explore the optical materials with large birefringence for the development of science and technology.

Based on the structure-property relationship in birefringent crystals, scientists generally believe that introducing functional units with high polarization anisotropy is conducive to the development of materials with large birefringence [13,14]. Stereochemically active lone pair cations, such as Sn^{2+}, I^{5+}, Te^{4+}, and Se^{4+}, as well as d^0 transition metal (TM) cations like V^{5+}, Mo^{6+}, W^{6+}, often exhibit significant polarization anisotropy, which favors enhanced birefringence [15,16]. As a result, a series of compounds with large birefringence, including, $Sn_9O_4Br_9Cl$ (0.273@1064 nm) [17], $CaYF(SeO_3)_2$ (0.127@1064 nm) [18], $ZrF_2(IO_3)_2$ (0.329@1064 nm) [19] and $LiGa(IO_3)_4$ (0.23@1064 nm) [20], have been synthesized. Moreover, d^{10}-TM like Zn^{2+}, Cd^{2+}, and Hg^{2+}, with their highly polarizable and deformable 18-electron configurations, can also significantly enhance birefringence [21,22]. For instance, compounds such as $HgTeO_2F(OH)$ (0.09@1064 nm) [23], $H_{11}C_4N_2CdI_3$ (0.090@546 nm) [24] and $LiZn(OH)CO_3$ (0.147@1064 nm) [25] display notable birefringence. Among them, Hg has garnered considerable attention due to its versatile coordination geometries and oxidation states. For example, Hg^I exhibits a linear O–Hg-Hg-O coordination [26,27], while Hg^{II} can adopt trigonal HgO_3, tetrahedral HgO_4, square-planar HgO_4, octahedral HgO_6 and polyhedral HgO_n coordination environments [28–33]. This diversity and flexibility in structure enable the discovery of a broad range of birefringent crystals.

Our group has conducted systematic research on the Hg-based tellurite system and successfully synthesized a series of compounds with excellent properties, such as $Hg_2(TeO_3)(SO_4)$ (0.146@546 nm), $Hg_3(Te_3O_8)(SO_4)$ (0.182@546 nm), $Hg^I_2Hg^{II}(Te_2O_4)_2(HPO_4)_2$ (0.444@546 nm) [26], and $Hg_4(Te_2O_5)(SO_4)$ (0.542@546 nm) [27]. Notably, $Hg_4(Te_2O_5)(SO_4)$ represents the largest birefringence reported among inorganic oxysalts. Se^{4+}, which is stereo-chemically similar to Te^{4+} in the same main group, also possesses active lone pairs. Combining Se^{4+} with Hg often results in compounds with large birefringence. However, within this system, only

* Corresponding author.
E-mail address: kongfang@fjirsm.ac.cn (F. Kong).

https://doi.org/10.1016/j.cclet.2024.110588
1001-8417/© 2025 Published by Elsevier B.V. on behalf of Chinese Chemical Society and Institute of Materia Medica, Chinese Academy of Medical Sciences.

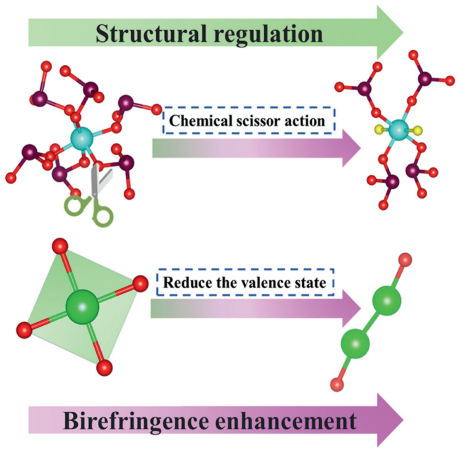


Fig. 1. Design roadmap for $Hg_2Ga(SeO_3)_2F$.

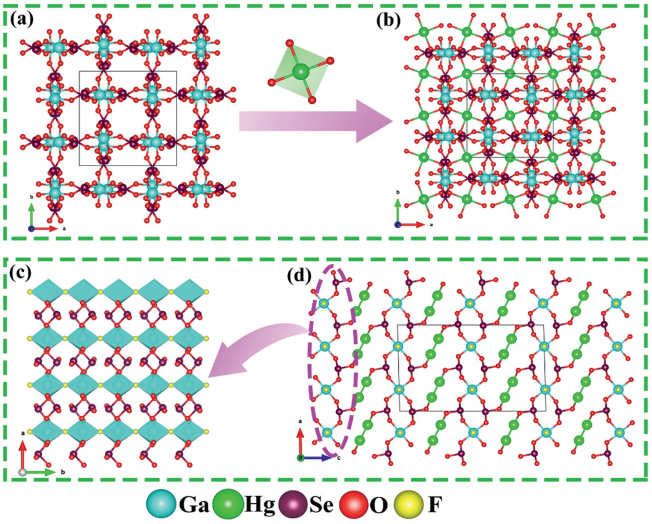


Fig. 2. (a) The 3D mercury selenate structure, (b) 3D structure of $HgGa_2(SeO_3)_4$. (c) The 2D gallium selenite layered structure and (d) 3D structure of $Hg_2Ga(SeO_3)_2F$.

three compounds have been reported with birefringence exceeding 0.1: $Hg_3(SeO_3)_2(SO_4)$ [28], $Hg_2(SeO_3)(SO_4)$ [32], and $MgHg(SeO_3)_2(H_2O)_2$ [34]. Therefore, systematic research in this area is essential. Based on this, we initially explored the Hg-Se-O system and successfully synthesized a NCS compound, $HgGa_2(SeO_3)_4$. This compound exhibits 60% of the SHG efficiency of commercial KDP; however, its birefringence is only 0.032@546 nm. Structural analysis revealed that the highly symmetric HgO_4 square-planar and GaO_6 octahedral coordination environments contribute minimally to birefringence. To overcome this limitation, we proposed introducing linear groups and fluoride ions to optimize the structure, thereby achieving enhanced birefringence [35]. The intended purpose of introducing fluoride ions is to reduce the coordination between the GaO_6 and SeO_3 groups, thereby enhancing the synergistic effect of the SeO_3 group. Meanwhile, the introduction of the linear Hg_2O_2 group aims to maximize the birefringence of the compound (Fig. 1). Guided by the above ideas, we successfully synthesized $Hg_2Ga(SeO_3)_2F$. Notably, $Hg_2Ga(SeO_3)_2F$ is the first reported Hg^I-based selenite birefringent material and exhibits excellent transparency in the MIR region. Herein, we provide a detailed description of the synthesis, crystal structure, thermal stability, and optical properties of these compounds.

$HgGa_2(SeO_3)_4$ and $Hg_2Ga(SeO_3)_2F$ have been synthesized through hydrothermal reactions at 200 °C. Detailed synthetic methods can be found in Synthesis section in Supporting information. The purities of the obtained products were confirmed using powder X-ray diffraction (PXRD), as shown in Fig. S1 (Supporting information).

The $HgGa_2(SeO_3)_4$ crystallizes in the NCS space group *I*-42*d*. The asymmetric unit of the crystal is composed of one selenium atom, one gallium atom, one mercury atom, and three oxygen atoms. Mercury and gallium atoms occupy special positions with occupancies of 0.25 and 0.5, respectively. The selenium atom is connected to three oxygen atoms to form a SeO_3 trigonal pyramid structure, while the gallium atom is coordinated with six oxygen atoms in an octahedral configuration. The Se-O bond lengths range from 1.682 Å to 1.715 Å, and the Ga-O bond lengths vary between 1.955 Å and 1.999 Å. The mercury atom, in a divalent state, is connected to four oxygen atoms, forming a planar square structure with each Hg-O bond length being 2.269 Å. According to the bond valence calculation results presented in Table S2 (Supporting information), the oxidation states of selenium, gallium, and mercury are +4, +3, and +2, respectively.

$HgGa_2(SeO_3)_4$ exhibits a complex three-dimensional (3D) structure composed of a 3D gallium selenite framework and HgO_4 planar square units (Fig. 2). In this structure, isolated GaO_6 octahedra are aligned along the a, b, and c axes of the crystal, with each GaO_6 octahedron connected to six SeO_3 groups (Fig. S2 in Supporting information). The SeO_3 groups act as linkers in this structure, bridging the isolated GaO_6 octahedra to form a continuous 3D gallium selenite framework (Fig. 2a). Meanwhile, the HgO_4 planar square units are nestled within the voids of this framework, providing stability to the entire structure (Fig. 2b).

Upon substituting Hg^{II} with Hg^I in $HgGa_2(SeO_3)_4$, along with partial fluorination of the GaO_6 octahedra, a new fluorinated selenite $Hg_2Ga(SeO_3)_2F$ is synthesized. This novel $Hg_2Ga(SeO_3)_2F$ compound crystallizes in the CS *I*2/*a* space group. Its asymmetric unit comprises one mercury atom, one selenium atom, one gallium atom, one fluorine atom, and three oxygen atoms, totaling seven atoms. In this structure, gallium and fluorine atoms occupy special positions, each with an occupancy rate of 0.5. The SeO_3 groups maintain their trigonal pyramidal configuration with Se-O bond lengths ranging from 1.706 Å to 1.713 Å. The gallium atom is coordinated with four oxygen atoms and two fluorine atoms, forming an octahedral configuration with Ga-O/F bond lengths between 1.931 Å and 1.967 Å. The mercury atom exists in the form of Hg^+, manifesting as Hg^{2+}, and forms a dumbbell-shaped configuration. Disregarding the longer Hg-O bonds, Hg(1)-Hg(1) is bridged by two oxygen atoms, forming a linear O(1)-Hg(1)-Hg(1)-O(1) group. The bond valences of selenium, mercury, and gallium are calculated to be 3.956, >0.569, and 2.948, respectively, indicating their oxidation states are +4, +1, and +3.

$Hg_2Ga(SeO_3)_2F$ exhibits a 3D structure composed of 2D gallium selenite layers and linear Hg_2O_2 units (Fig. 2). In this structure, multiple GaO_4F_2 octahedra share F atoms to form straight chains of gallium octahedra (Fig. S3 in Supporting information). This type of structure has also been observed in our previously reported compound, $Pb_2Ga_3F_3(Te_6F_2O_{16})$ [36]. The SeO_3 groups bridge these straight chains of gallium octahedra, creating 2D gallium selenite layers (Fig. 2c). The linear Hg_2O_2 units further connect these layers, forming the overall 3D structure of the compound (Fig. 2d).

Within the temperature range of 20–800 °C, thermal gravimetric analysis (TGA) was conducted on $HgGa_2(SeO_3)_4$ and $Hg_2Ga(SeO_3)_2F$. $HgGa_2(SeO_3)_4$ demonstrated good thermal stability up to 300 °C. Upon reaching 800 °C, the observed weight loss corresponded to the theoretical loss of 4 molecules of SeO_2 and 1 molecule of HgO. The experimental weight loss was measured at 76.1%, which is very close to the theoretically calculated value of

77.8 % (Fig. S4a in Supporting information). As for $Hg_2Ga(SeO_3)_2F$, it remained stable below 200 °C. At 800 °C, the weight loss was primarily attributed to the evaporation of 1 molecule of F, 2 molecules of SeO_2, and 1 molecule of Hg_2O. The experimental weight loss was 88.4 %, which matches the theoretical weight loss of 88.5 % (Fig. S4b in Supporting information). The thermal stability of $Hg_2Ga(SeO_3)_2F$ is slightly lower than that of $HgGa_2(SeO_3)_4$, mainly due to the presence of fluorine atoms.

The infrared (IR) spectra of $HgGa_2(SeO_3)_4$ and $Hg_2Ga(SeO_3)_2F$ were measured at room temperature, covering the wavelength range of 4000–400 cm^{-1} (Fig. S5 in Supporting information). No absorption peaks were detected for either compound between 4000 cm^{-1} and 900 cm^{-1}. The absorption peaks observed between 405 cm^{-1} and 470 cm^{-1}, as well as 650 and 850 cm^{-1} for both compounds, can be attributed to the characteristic vibrations of the $(SeO_3)^{2-}$ group. The vibrational peaks corresponding to the Ga-O group are found in the range of 410–530 cm^{-1}, consistent with values reported in the literature [37–39].

UV/Vis-NIR absorption spectroscopy analysis shows that the UV cutoff edges of $HgGa_2(SeO_3)_4$ and $Hg_2Ga(SeO_3)_2F$ are approximately 273 nm and 383 nm, respectively, corresponding to band gaps of 4.0 eV and 2.8 eV (Fig. S6 in Supporting information). For $HgGa_2(SeO_3)_4$, its band gap is larger than those of previously reported mercury-based selenites, such as $Ag_4Hg(SeO_3)_2(SeO_4)$ (3.11 eV) [30], $Hg_3Se(SeO_3)(SO_4)$ (3.58 eV) [39], $K_2Hg_2(SeO_3)_3$ (3.64 eV) [31], and $Hg_2(SeO_3)(SO_4)$ (3.58 eV) [32]. Meanwhile, the band gap of $Hg_2Ga(SeO_3)_2F$ is comparable to that of previously reported Hg^I-based compounds, such as $Hg_4(Te_2O_5)(SO_4)$ (2.85 eV) [27]. The powdered crystals of $HgGa_2(SeO_3)_4$ and $Hg_2Ga(SeO_3)_2F$ exhibit wide transparency ranges, spanning from 0.27 μm to 11.5 μm and 0.38–12.3 μm, respectively. To account for the discrepancies in the IR cutoff edge observed between powder and crystal measurements, which are largely attributed to multiphonon absorption, a 50 % correction has been applied [40,41]. With this adjustment, the transparency ranges for $HgGa_2(SeO_3)_4$ and $Hg_2Ga(SeO_3)_2F$ are refined to 0.27–5.8 μm and 0.38–6.2 μm, respectively. These ranges cover crucial atmospheric transparency windows in the MIR region, indicating that these materials are promising candidates MIR birefringent materials.

Second-harmonic generation (SHG) measurements reveal that $HgGa_2(SeO_3)_4$ particles with ranging from 150 μm to 210 μm can exhibit SHG signals under 1064 nm laser irradiation, which are approximately 60 % of that of commercially available KDP (Fig. 3a). Tests with particles of varying sizes demonstrate that the SHG intensity increases with particle size, indicating phase matching (Fig. 3b). Notably, $HgGa_2(SeO_3)_4$ is the first example of a Hg-based simple selenite exhibiting SHG intensity. Structural analysis indicates that the SHG effect primarily stems from the contribution of the SeO_3 groups. It is noteworthy that the SHG effect of $HgGa_2(SeO_3)_4$ is greater than that of the $Ag_4Hg(SeO_3)_2(SeO_4)$ we previously reported (0.35 × KDP) [30], and comparable to that of $Cd_3(SeO_3)_2(SeO_4)$ (0.6 × KDP) and $Hg_3(SeO_3)_2(SeO_4)$ (0.8 × KDP) [42].

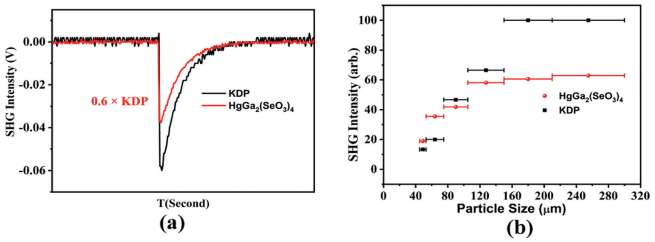


Fig. 3. (a) The oscilloscope traces of the SHG signal, and (b) the measured SHG signals with different particle sizes for $HgGa_2(SeO_3)_4$.

To gain deeper insights into the electronic properties of $HgGa_2(SeO_3)_4$ and $Hg_2Ga(SeO_3)_2F$, theoretical calculations were performed using the DFT method for both compounds. As shown in Fig. S7 (Supporting information), both compounds are direct bandgap materials, with calculated bandgaps of 3.022 eV and 2.614 eV, respectively. Due to the limitations of theoretical calculations, the calculated bandgaps are generally smaller than the experimental values [43,44]. Therefore, in the subsequent analysis, scissor corrections of 0.978 eV and 0.186 eV were applied to the two compounds, respectively.

The total and partial density of states (DOS) for $HgGa_2(SeO_3)_4$ and $Hg_2Ga(SeO_3)_2F$ are shown in Fig. S8 (Supporting information), and both compounds exhibit similar DOS characteristics. The top of the valence bands (VBs) is mainly dominated by O-2p and Se-4p orbitals, while the conduction bands (CBs) close to the Fermi level are primarily composed of Se-4p and Hg-6s states. Therefore, the bandgaps of these compounds are mainly determined by the contributions from Hg, Se, and O atoms.

The birefringence of these two compounds was calculated based on the formula $\varepsilon(\omega) = \varepsilon_1(\omega) + i\varepsilon_2(\omega)$ and $n^2(\omega) = \varepsilon(\omega)$. $HgGa_2(SeO_3)_4$ is a uniaxial crystal, where the extraordinary refractive index n_e is greater than the ordinary refractive index n_o. The birefringence (Δn) values for the material are 0.032@546 nm, 0.028@1064 nm and 0.027@2000 nm (Fig. 4a). These values are similar to those observed in $Y_3F(SeO_3)_4$, which has a birefringence of 0.038@532 nm [18], and in $NaGa_3(HSeO_3)_6(SeO_3)_2$, with a birefringence of 0.033@532 nm [45]. Additionally, $Hg_2Ga(SeO_3)_2F$, identified as a biaxial crystal, demonstrates birefringence values of 0.111@546 nm, 0.095@1064 nm and 0.091@2000 nm (Fig. 4b). Fig. 4c and Table S4 (Supporting information) summarized the birefringence data of Hg-based selenites reported in the literature. Notably, $Hg_2Ga(SeO_3)_2F$ shows a large birefringence and is the first example of Hg^I-based selenite birefringent material. It is worth mentioning that $Hg_2Ga(SeO_3)_2F$ has a wide transmission window, indicating its potential as a MIR birefringent material.

Compared to $HgGa_2(SeO_3)_4$, the birefringence of $Hg_2Ga(SeO_3)_2F$ has been enhanced by 3.5 times. Therefore, it is necessary to analyze the reasons behind the differences in birefringence between these two compounds. For $HgGa_2(SeO_3)_4$, its smaller birefringence is mainly due to the following factors: As shown in Figs. 5a and b and Table S2 (Supporting information), the highly symmetrical configurations of the GaO_6 octahedron and HgO_4 square contribute almost nothing to the birefringence. Although the lone pair electrons in the SeO_3 group have a positive effect on birefringence, the SeO_3 group is connected to six oxygen atoms in the highly symmetrical GaO_6 octahedron (Fig. 5a). This causes the lone pair electrons to be arranged in different directions, resulting in the birefringence canceling out, thus leading to a smaller overall birefringence in this compound. For $Hg_2Ga(SeO_3)_2F$, its large birefringence is mainly attributed to the introduction of the linear Hg_2O_2 group. Compared to the planar HgO_4 square, the Hg_2O_2 group exhibits more large anisotropy, and in this structure, the linear Hg_2O_2 groups are arranged in an orderly manner along the same direction. Additionally, due to the "chemical scissor" effect of fluorine atoms [46], partial fluorination of the GaO_6 octahedra prevents the anisotropy of the SeO_3 groups from canceling each other out. According to literature, for linear groups, the direction of maximum refractive index is parallel to the linear structure of the molecule, while for lone-pair electron groups, the direction of maximum refractive index is perpendicular to the orientation of the lone pair, which usually points toward the direction of minimum refractive index [47]. As shown in Figs. 5c and d, the synergistic effect between the linear Hg_2O_2 group and the lone-pair SeO_3 group results in the large birefringence observed in this compound.

In summary, two new selenite compounds, $HgGa_2(SeO_3)_4$ and $Hg_2Ga(SeO_3)_2F$, were successfully synthesized in the Hg-based se-

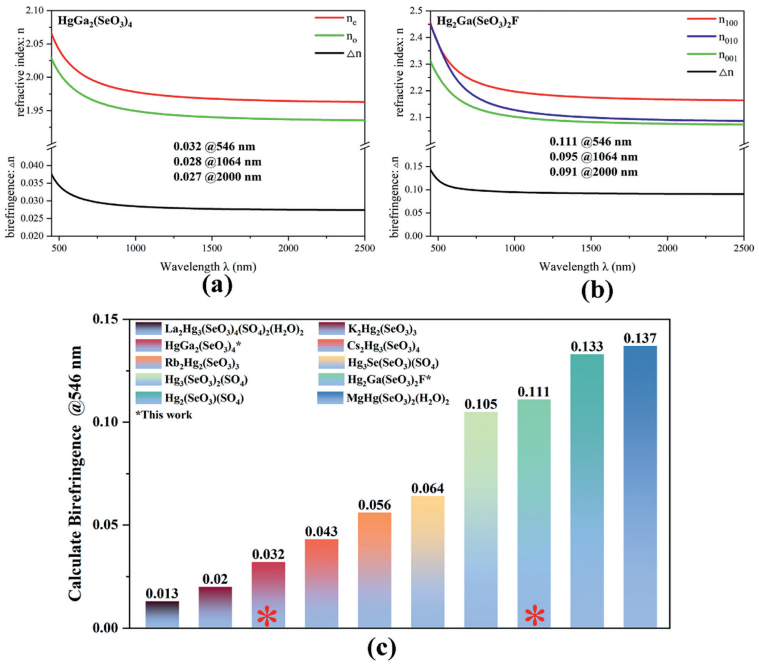


Fig. 4. The calculated refractive indices and birefringence values of (a) $HgGa_2(SeO_3)_4$ and (b) $Hg_2Ga(SeO_3)_2F$. (c) The birefringence of the reported Hg-based selenite crystals.

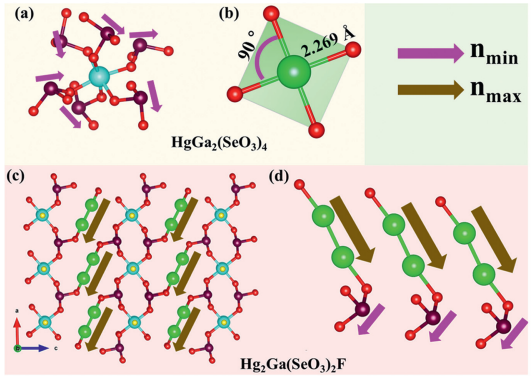


Fig. 5. (a, b) The schematic diagram illustrating the cancellation of effects in $HgGa_2(SeO_3)_4$. (c, d) The Schematic diagram of the synergistic effect in $Hg_2Ga(SeO_3)_2F$.

lenite system using a mild hydrothermal method. $HgGa_2(SeO_3)_4$ crystallizes in a NCS space group and represents the first example of a Hg-based simple selenite with SHG intensity. It exhibits 60 % of the SHG intensity of commercial KDP, along with good stability, a large bandgap (4.0 eV), and a broad transmission window (0.27–5.8 μm). $Hg_2Ga(SeO_3)_2F$ represents the first Hg^I-based selenite birefringent material, showing a large birefringence (0.111@546 nm) and wide transmission window (0.38–6.2 μm), making it a promising candidate for birefringent applications. Structural analysis reveals that the large birefringence of $Hg_2Ga(SeO_3)_2F$ arises from the synergistic effect of the linear Hg_2O_2 and SeO_3 groups. Our work presents a novel approach for designing new birefringent materials. Next, we will conduct a more systematic investigation of the Hg^I-based selenite system.

Declaration of competing interest

The authors declare that they have no known competing financial interests or personal relationships that could have appeared to influence the work reported in this paper.

CRediT authorship contribution statement

Peng-Fei Li: Writing – original draft, Methodology, Investigation, Formal analysis, Data curation. **Chun-Li Hu:** Software, Methodology. **Bo Zhang:** Data curation. **Jiang-Gao Mao:** Supervision, Resources, Funding acquisition. **Fang Kong:** Writing – review & editing, Supervision, Resources, Funding acquisition.

Acknowledgments

This work was supported by the National Natural Science Foundation of China (Nos. 22475215, 22031009 and 21921001), the NSF of Fujian Province (Nos. 2023J01216, 2024J010039) and the Self-deployment Project Research Program of Haixi Institutes, Chinese Academy of Sciences (No. CXZX-2022-GH06).

Supplementary materials

Supplementary material associated with this article can be found, in the online version, at doi:10.1016/j.cclet.2024.110588.

References

[1] H.Y. Sha, Y.R. Shang, Z.J. Wang, et al., Small 20 (2023) e2309776.
[2] J. Chen, M.B. Xu, H.Y. Wu, et al., Angew. Chem. Int. Ed. 63 (2024) e202411503.
[3] H. Sha, D. Yang, Y. Shang, et al., Chin. Chem. Lett. 36 (2025) 109730.
[4] M. Ma, J. Dang, Y. Wu, et al., Inorg. Chem. 62 (2023) 6549–6553.
[5] G. Ghosh, Opt. Commun. 163 (1999) 95–102.
[6] H.T. Luo, T. Tkaczyk, E.L. Dereniak, et al., Opt. Lett. 31 (2006) 616–618.
[7] M.J. Dodge, Appl. Opt. 23 (1984) 1980–1985.
[8] J.R. DeVore, J. Opt. Soc. Am. 41 (1951) 416–419.
[9] D.E. Zelmon, D.L. Small, D. Jundt, J. Opt. Soc. Am. 14 (1997) 3319–3322.
[10] S.J. Han, A. Tudi, W.B. Zhang, et al., Angew. Chem. Int. Ed. 62 (2023) e202302025.
[11] Y. Lan, J. Ren, P. Zhang, et al., Chin. Chem. Lett. 35 (2024) 108652.
[12] D. Yan, M.M. Ren, Q. Liu, et al., Inorg. Chem. 62 (2023) 4757–4761.
[13] Z. Hu, L. Liu, R. Zhang, et al., J. Mater. Chem. C 11 (2023) 3325–3333.
[14] B. Zhang, M.Y. Ran, X.T. Wu, et al., Coord. Chem. Rev. 517 (2024) 216053.
[15] X.H. Dong, H.B. Huang, L. Huang, et al., Angew. Chem. Int. Ed. 63 (2024) e202318976.
[16] M.B. Xu, Q.Q. Chen, B.X. Li, et al., Chin. Chem. Lett. 36 (2025) 110513.
[17] M. Hu, C. Tu, Z. Yang, et al., Scripta Mater 231 (2023) 115437.
[18] P.F. Li, C.L. Hu, F. Kong, et al., Angew. Chem. Int. Ed. 62 (2023) e202301420.
[19] J. Chen, K.Z. Du, Inorg. Chem. 61 (2022) 17893–17901.

[20] S. Yang, H. Wu, Z. Hu, et al., Small 20 (2023) 2306459.
[21] Y. Li, K.M. Ok, Angew. Chem. Int. Ed. 63 (2024) e202409336.
[22] J. Zhou, Z. Fan, K. Zhang, et al., Mater. Horiz. 10 (2023) 619–624.
[23] R.L. Tang, M. Yan, W.D. Yao, et al., Inorg. Chem. 61 (2022) 2333–2339.
[24] H.Y. Wu, C.L. Hu, M.B. Xu, et al., Chem. Sci. 14 (2023) 9533–9542.
[25] X. Liu, L. Kang, P. Gong, et al., Angew. Chem. Int. Ed. 60 (2021) 13574–13578.
[26] P.F. Li, C.L. Hu, J.G. Mao, et al., Laser Photonics Rev. 19 (2025) 2401488.
[27] P.F. Li, C.L. Hu, Y.F. Li, et al., J. Am. Chem. Soc. 146 (2024) 7868–7874.
[28] J. Ren, Y. Chen, L. Ren, et al., Inorg. Chem. 62 (2023) 9130–9138.
[29] M.Y. Ran, S.H. Zhou, W.B. Wei, et al., Small 20 (2024) 2304563.
[30] X.X. Wang, X.B. Li, C.L. Hu, et al., Sci. China Mater. 62 (2019) 1821–1830.
[31] J. Ren, H. Cui, L. Cheng, et al., Inorg. Chem. 62 (2023) 21173–21180.
[32] P.F. Li, C.L. Hu, F. Kong, et al., Mater. Chem. Front. 6 (2022) 3567–3576.
[33] J. Chen, C. Lin, X. Jiang, et al., Mater. Horiz. 10 (2023) 2876–2882.
[34] Y.L. Sun, L. Huai, A.H. Gong, J. Solid State Chem. 336 (2024) 124772.
[35] Z. Yan, J. Fan, S. Pan, et al., Chem. Soc. Rev. 53 (2024) 6568–6599.
[36] P.F. Li, J.G. Mao, F. Kong, Mater. Today Phys. 37 (2023) 101197.
[37] J. Zhang, H. Yu, Z. Hu, et al., Mater. Today Phys. 35 (2023) 101145.
[38] G. Park, K.M. Ok, Inorg. Chem. Front. 7 (2020) 4469–4476.
[39] P.F. Li, C.L. Hu, B.X. Li, et al., Inorg. Chem. 63 (2024) 4011–4016.
[40] P.F. Li, C.L. Hu, B.X. Li, et al., Inorg. Chem. Front. 10 (2023) 7343–7350.
[41] Z. Yang, C. Hu, M. Mutailipu, et al., J. Mater. Chem. C 6 (2018) 2435–2442.
[42] M. Shang, P.S. Halasyamani, J. Solid State Chem. 286 (2020) 121292.
[43] M. Yan, R.L. Tang, W.D. Yao, et al., Chem. Sci. 15 (2024) 2883–2888.
[44] M.Y. Ran, S.H. Zhou, X.T. Wu, et al., Mater. Today Phys. 44 (2024) 101442.
[45] P.F. Li, C.L. Hu, J.G. Mao, et al., Coord. Chem. Rev. 517 (2024) 216000.
[46] P.F. Li, C.L. Hu, J.G. Mao, et al., Chem. Sci. 15 (2024) 7104–7110.
[47] J.Y. Guo, A. Tudi, S.J. Han, et al., Angew. Chem. Int. Ed. 60 (2021) 3540–3544.